Inorg. Chem. **2007**, *46*, 7050–7054

Synthesis of an Octanuclear Eu(III) Cage from Eu_4^{2+}: Chloride Anion Encapsulation, Luminescence, and Reversible MeOH Adsorption via a Porous Supramolecular Architecture

Xiaoping Yang,[†] Benjamin P. Hahn,[†] Richard A. Jones,*[,†] Wai-Kwok Wong,*[,‡] and Keith J. Stevenson*[,†]

Department of Chemistry and Biochemistry, The University of Texas, 1 University Station A5300, Austin, Texas 78712-0165, and Department of Chemistry, Hong Kong Baptist University, Kowloon Tong, Hong Kong, P. R. China

Received May 5, 2007

The octanuclear complex $[Eu_8L_4(1,4\text{-BDC})_2Cl_8(MeOH)_{12}]\cdot 4Cl\cdot 2MeOH\cdot 18H_2O$ (**2**) was obtained from the reaction of the tetranuclear Eu(III) species $[Eu_4L_2Cl_2(OH)_4(H_2O)_4(MeOH)_2]\cdot 2Cl\cdot 7MeOH\cdot 2H_2O$ (**1**) and 1,4-H_2BDC (H_2L = bis-(5-bromo-3-methoxysalicylidene)ethylene-1,2-phenylenediamine, 1,4-H_2BDC = 1,4-benzenedicarboxylic acid). Both **1** and **2** were structurally characterized by X-ray crystallography, and their luminescence properties were determined. The cagelike structure of **2** encapsulates two chloride anions via MeOH···Cl hydrogen bonding. In the solid state, **2** has an open three-dimensional network with extended channels and is capable of reversible MeOH adsorption.

Introduction

Polynuclear metal complexes are currently of interest for potential applications in optoelectronics and magnetism and as porous materials.[1] For the d-block transition metals, a variety of macrocycles, cages, and polyhedra can be prepared using nitrogen-containing heteroaryls, cyano-substituted aromatics, *o*-catecholamides, hydroxamates, and phosphorus-containing ligands.[2] In contrast, the rational design and synthesis of polynuclear lanthanide complexes is more challenging and far less developed. This may be caused by the difficulty in controlling the coordination environment of the Ln(III) ions which often display high and variable coordination numbers.[3] We recently described a straightforward strategy directed toward the rational structural design of polynuclear lanthanide complexes. This involves the use of two different ligands: one to coordinate Ln(III) ions and the other to act as a linker between suitably ligated metal units.[4] In this case, we successfully constructed a hexanuclear Zn_4Nd_2 prism $[Zn_4Nd_2L_4(1,4\text{-BDC})_2]^{2+}$ using a "salen-style" Schiff-base ligand with 1,4-benzenedicarboxylate (1,4-BCD) units. We describe here the further implementation of the two-ligand approach with the synthesis of a luminescent octanuclear Eu(III) complex $[Eu_8L_4(1,4\text{-BDC})_2Cl_8(MeOH)_{12}]\cdot 4Cl\cdot 2MeOH\cdot 18H_2O$ (**2**), constructed from two units of a tetranuclear Eu(III) complex $[Eu_4L_2Cl_2(OH)_4(H_2O)_4(MeOH)_2]\cdot$

* To whom correspondence should be addressed. Phone: (512) 471-1706 (R. A. J.); 852-3411-7011 (W.-K. W.). E-mail: rajones@mail.utexas.edu (R. A. J.); wkwong@hkbu.edu.hk (W.-K. W.); stevenson@cm.utexas.edu (K. J. S.).

[†] The University of Texas at Austin.

[‡] Hong Kong Baptist University.

(1) (a) *Clusters and Colloids*: *From Theory to Applications*; Schmidt G., Ed.; VCH: Weinheim, Germany, 1994. (b) Lehn, J. M. *Supramolecular Chemistry*: *Concepts and Perspectives*; VCH: Weinheim, Germany, 1995. (c) Vigato, P. A.; Tamburini, S. *Coord. Chem. Rev.* **2004**, *248*, 1717. (d) Bünzli, J.-C. G.; Piguet, C. *Chem. Rev.* **2002**, *102*, 1897. (e) Zanello, P.; Tamburini, S.; Vigato, P. A.; Mazzocchin, G. A. *Coord. Chem. Rev.* **1987**, *77*, 165. (f) Alivisatos, A. P. *J. Phys. Chem.* **1996**, *100*, 13226. (g) Huignard, A.; Gacoin, T.; Boilot, J. P. *Chem. Mater.* **2000**, *12*, 1090. (h) Faulkner, S.; Pope, S. J. A.; Burton-Pye, B. P. *Appl. Spectrosc. Rev.* **2005**, *40*, 1.

(2) (a) Leininger, S.; Olenyuk, B.; Stang, P. J. *Chem. Rev.* **2000**, *100*, 853. (b) Zheng, Z. *Chem. Commun.* **2001**, 2521 and references therein. (c) Caneschi, A.; Cornia, A.; Fabretti, A. C.; Gatteschi, D. *Angew. Chem., Int. Ed.* **1999**, *38*, 1295. (d) Bhula, R.; Weatherburn, D. C. *Angew. Chem., Int. Ed. Engl.* **1991**, *30*, 688. (e) Cavalluzzo, M.; Chen, Q.; Zubieta, J. *Chem. Commun.* **1993**, 131. (f) Steunou, N.; Bonhomme, C.; Sanchez, C.; Vaissermann, J.; Hubert-Pfalzgraf, L. J. *Inorg. Chem.* **1998**, *37*, 901. (g) Mehrotra, R. C.; Singh, A.; Sogani, S. *Chem. Soc. Rev.* **1994**, *23*, 215. (h) Benelli, C.; Caneschi, A.; Gatteschi, D.; Pardi, L. *Magnetic Molecular Materials*; Gatteschi, D., Ed.; NATO ASI Series 198; Kluwer Academic: Dordrecht, The Netherlands, 1991. (i) Anwander, R. *Angew. Chem., Int. Ed. Engl.* **1998**, *37*, 599.

(3) (a) Bünzli, J.-C. G. *Lanthanides Probes in Life, Chemical and Earth Sciences*; Elsevier: Amsterdam, The Netherlands, 1989; Vol. 1989. (b) Piguet, C.; Bünzli, J.-C. G. *Chem. Soc. Rev.* **1999**, *28*, 347.

(4) (a) Yang, X.-P.; Jones, R. A.; Wong, W.-K.; Lynch, V.; Oye, M. M.; Holmes, A. L. *Chem. Commun.* **2006**, 1836. (b) Yang, X.-P.; Jones, R. A. *J. Am. Chem. Soc.* **2005**, *127*, 7686. (c) Wong, W.-K.; Yang, X.-P.; Jones, R. A.; Rivers, J. H.; Lynch, V.; Lo, W.-K.; Xiao, D.; Oye, M. M.; Holmes, A. L. *Inorg. Chem.* **2006**, *45*, 4340.

10.1021/ic7008682 CCC: $37.00
Published on Web 07/11/2007

Scheme 1. Formation of the Octanuclear Eu(III) Cage **2**

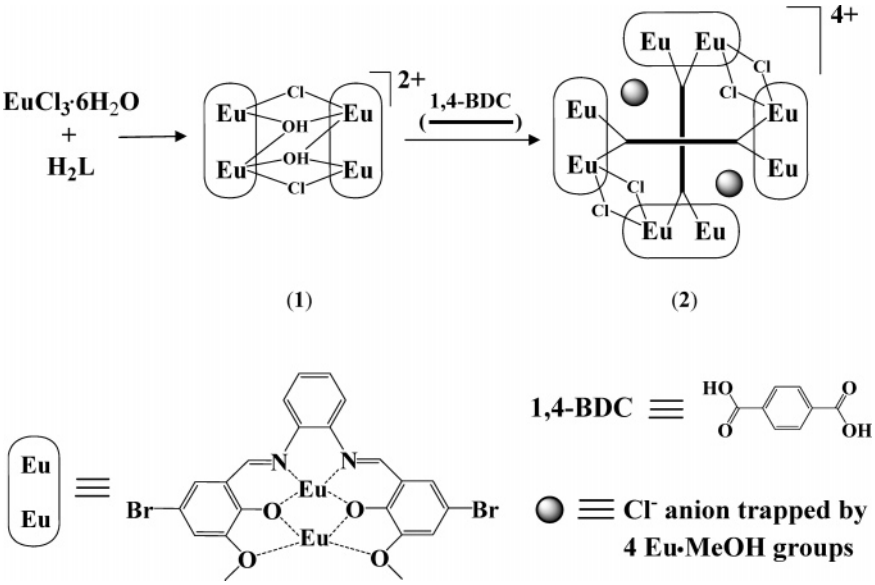

2Cl·7MeOH·2H_2O (**1**) and 1,4-BDC groups (Scheme 1). The central Eu_8^{4+} core of **2** has a distorted cubelike structure in the solid state and encapsulates two Cl^- anions simply via hydrogen bonding with coordinated MeOH molecules.[5] In the solid state, **2** forms a supramolecular 3-D open network structure which allows for the reversible adsorption of small organic molecules such as MeOH. Although numerous lanthanide derivatives of salen-type ligands have been described, most are poorly characterized and are of relatively low nuclearity.[6] To the best of our knowledge, **2** is the first example of an octanuclear Ln(III) salen cage.

Experimental Section

All reactions were performed under dry oxygen-free dinitrogen atmospheres using standard Schlenk techniques. Metal salts and solvents were purchased from Aldrich. Solvents for the photophysical investigations were dried over molecular sieves and freshly distilled under dry nitrogen before use. Physical measurements: ESI mass spectroscopy, Finnigan MAT TSQ 700; NMR, Varian 300 Unity Plus spectrometer (^{1}H, 300 MHz) at 298 K (chemical shifts referenced to the deuterated solvent); IR, Nicolet IR 200 FT-IR spectrometer. The absorption spectra were obtained on a BECKMAN DU 640 spectrophotometer, and the excitation and visible emission spectra were obtained on a QuantaMaster PTI fluorimeter.

Synthesis of [$Eu_4L_2Cl_2(OH)_4(H_2O)_4(MeOH)_2$]·2Cl·7MeOH·2$H_2O$ (1). Triethylamine (10 mL of 0.1 M MeCN solution) was added to a solution of H_2L (0.265 g, 0.50 mmol) and $EuCl_3·6H_2O$ (0.365 g, 1 mmol) in 50 mL of MeOH. The mixture was stirred and refluxed for 30 min, cooled to room temperature, and filtered. Diethyl ether was allowed to diffuse slowly into this solution at room temperature, and pale yellow single crystals were obtained in one month. Yield: 0.367 g (66%). ESI-MS (CH_3OH): *m*/*z* 930 [M − 2Cl^- − 6MeOH]$^{2+}$. IR (CH_3OH, cm^{-1}): ν 3302 (s), 1622 (s), 1500 (s), 1455 (m), 1379 (m), 1312 (m), 1266 (m), 1037 (s), 1242 (m), 1032 (m), 961 (m), 778 (m), 660 (m), 590 (m).

Synthesis of [Eu_8L_4(1,4-BDC)$_2Cl_8(MeOH)_{12}$]·4Cl·2MeOH·18H_2O (2). Triethylamine (2 mL of 0.1 M MeCN solution) was added to a solution of **1** (0.216 g, 0.10 mmol) and 1,4-BDC (0.017 g, 0.10 mmol) in 30 mL of MeOH. The resulting solution was stirred and refluxed for 10 h. After filtration, the solution was left standing in air, and yellow single crystals of **1** were obtained after three weeks. Yield: 0.145 g (61%, based on 1,4-BDC). ESI-MS (CH_3OH): *m*/*z* 1068 [M − 4Cl^- − 2MeOH − 14H_2O]$^{4+}$. ^{1}H NMR (400 MHz, CD_3CN): δ −0.587 (5H), 1.109 (5H), 2.585 (5H), 3.259 (1H), 3.410 (3H), 3.840 (3H), 4.205 (4H), 4.627 (2H), 5.726 (5H), 5.981 (3H), 6.704 (1H), 6.960 (1H), 7.025 (1H), 7.138 (2H), 7.461 (1H), 7.572 (4H), 7.619 (2H), 7.771 (1H), 8.335 (2H), 8.803 (1H), 10.906 (8H), 11.650 (2H), 17.392 (2H). IR (CH_3OH, cm^{-1}): ν 3378 (m), 3219 (m), 1635 (s), 1620 (s), 1562 (s), 1540 (m), 1508 (m), 1460 (m), 1442 (w), 1387 (m), 1370 (w), 1300 (m), 1237 (m), 1036 (s), 1291 (m), 1237 (m), 1031 (m), 960 (w), 779 (m), 662 (m), 597 (m), 496 (m).

Crystallographic Analyses. Data were collected on a Nonius Kappa CCD diffractometer with graphite-monochromated Mo Kα radiation (λ = 0.71073 Å) at 153 K. Absorption corrections were applied using GAUSSIAN. The structures were solved by direct methods and refined anisotropically using full-matrix least-squares methods with the SHELX 97 program package.[7] The coordinates of the non-hydrogen atoms were refined anisotropically, while the hydrogen atoms were included in the calculation isotropically but not refined. Neutral atom-scattering factors were taken from Cromer and Waber.[8] The crystallographic data and selected bond lengths for **1** and **2** are listed in Table 1. Selected bond lengths and angles for **1** and **2** are given in Tables 2 and 3, respectively.

QCM Studies. Gas-phase quartz crystal microbalance (QCM) experiments were conducted in a home-built chamber interfaced

(5) For a recent example of Cl^- coordinated by O-H···Cl hydrogen bonds in a lanthanide complex, see: (a) Omata, K.; Hoshi, N.; Kabuto, K.; Kabuto, C.; Sasaki, Y. *Inorg. Chem.* **2006**, *45*, 5263. (b) Custelcean, R.; Gorbunova, M. G. *J. Am. Chem. Soc.* **2005**, *127*, 16362. (c) Goetz, S.; Kruger, P. E. *Dalton Trans.* **2006**, 1277.

(6) (a) Hogerheide, M. P.; Boersma, J.; Konten, G. V. *Coord. Chem. Rev.* **1996**, *155*, 87. (b) Costes, J.-P.; Dupuis, A.; Laurent, J.-P. *Inorg. Chim. Acta* **1998**, *268*, 125. (c) Costes, J.-P.; Laussac, J.-P.; Nicodème, F. *J. Chem. Soc., Dalton Trans.* **2002**, 2731. (d) Liu, G.; Na, C.; Liu, B.; Mao, K. *Polyhedron* **1990**, *9*, 2019. (e) Chen, H.; Archer, R. D. *Inorg. Chem.* **1994**, *33*, 5195. (f) Xie, W.; Heeg, M. J.; Wang, P. G. *Inorg. Chem.* **1999**, *38*, 2541.

(7) Sheldrick, G. M. *SHELX 97, A software package for the solution and refinement of X-ray data*; University of Göttingen: Göttingen, Germany, 1997.

(8) Cromer, D. T.; Waber, J. T. *International Tables for X-Ray Crystallography*; Kynoch Press: Birmingham, U.K., 1974; Vol. 4, Table 2.2A.

Table 1. Crystal Data and Structure Refinement for Complexes **1** and **2**

	1	**2**
formula	$C_{52}H_{76}Br_4Cl_4Eu_4N_4O_{24}$	$C_{118}H_{156}Br_8Cl_{12}Eu_8N_8O_{52}$
fw	2210.45	4798.87
cryst syst	monoclinic	monoclinic
space group	$P2_1/c$	$C2/c$
a (Å)	15.491(3)	21.184(4)
b (Å)	19.933(4)	32.694(7)
c (Å)	15.115(3)	32.822(7)
β (deg)	114.09(3)	95.79(3)
V (Å^3)	4260.7(16)	22616(8)
Z	2	4
D_{calcd} (g cm^{-3})	1.723	1.409
temp (K)	153(1)	153(1)
F(000)	2136	9296
μ (mm^{-1})	4.967	3.796
θ range (deg)	3.17−25.00	3.19−25.00
reflns measured	14 576	35 995
reflns used	7379	18 968
params	433	949
R[a] ($I > 2\sigma(I)$)	R1 = 0.0908	R1 = 0.0876
	wR2 = 0.1561	wR2 = 0.1893
R[a] (all data)	R1 = 0.1926	R1 = 0.2098
	wR2 = 0.2206	wR2 = 0.2465
S	1.051	1.016

[a] $R1 = \sum||F_o| - |F_c||/\sum|F_o|$; $wR2 = [\sum w[(F_o^2 - F_c^2)^2]/\sum|[w(F_o^2)^2]]^{1/2}$; $w = 1/[\sigma^2(F_o^2) + (0.075P)^2]$, where $P = [\max(F_o^2,0) + 2F_c^2]/3$.

Table 2. Selected Bond Lengths (Å) and Angles (deg) for **1**

Eu(1)−O(5)	2.360(8)	O(3)−Eu(1)−N(1)	103.2(4)
Eu(1)−O(6)	2.384(11)	O(3)−Eu(1)−O(2)	69.6(3)
Eu(1)−O(5)#1	2.401(9)	N(1)−Eu(1)−O(2)	71.3(3)
Eu(1)−O(3)	2.420(9)	O(3)−Eu(1)−N(2)	71.7(3)
Eu(1)−N(1)	2.463(11)	N(1)−Eu(1)−N(2)	61.3(4)
Eu(1)−O(2)	2.471(11)	O(2)−Eu(1)−N(2)	107.3(4)
Eu(1)−N(2)	2.500(10)	O(3)−Eu(2)−O(2)	71.3(3)
Eu(1)−Cl(1)#1	2.717(5)	O(3)−Eu(2)−O(4)	61.2(3)
Eu(2)−O(7)	2.342(11)	O(2)−Eu(2)−O(4)	129.9(3)
Eu(2)−O(3)	2.362(9)	O(3)−Eu(2)−O(1)	122.7(3)
Eu(2)−O(8)	2.415(12)	O(2)−Eu(2)−O(1)	59.6(3)
Eu(2)−O(2)	2.423(8)	O(4)−Eu(2)−O(1)	138.7(4)
Eu(2)−O(5)	2.433(10)		
Eu(2)−O(9)	2.445(9)		
Eu(2)−O(4)	2.561(9)		
Eu(2)−O(1)	2.632(11)		
Eu(2)−Cl(1)	2.918(4)		

to a CH 440 time-resolved electrochemical quartz crystal microbalance (CH Instruments, Texas). Briefly, a solution of **1** (6×10^{-8} mol) in MeCN (0.5 mL) was drop-cast onto the working electrode portion of a 9.995 MHz gold−titanium AT-cut quartz crystal, and the solvent was removed under vacuum. The QCM crystal was then placed inside the chamber where it sat on an adjustable stage that could be pressed against an O-ring, and the entire moving platform was enclosed between two Teflon pieces that screwed into place. A glass covering fitted with a septum allowed for the direct injection of methanol into the cell in 1 μL increments with a 10 μL gastight syringe (Hamilton Co., Nevada). The QCM crystal was allowed to equilibrate overnight prior to experimentation. Additionally, no methanol injections occurred during the first 100 s of any QCM experiment; this time region was used to provide a baseline for the QCM crystal drift. After saturation, the crystal was removed from the cell and placed under vacuum to remove volatile components. The crystal was then replaced into the chamber, and the sorption process was repeated. The adsorption−desorption cycle was repeated at least three times.

Results and Discussion

Reaction of $EuCl_3 \cdot 6H_2O$ with H_2L in a 2:1 mole ratio in MeOH gave **1** in 68% yield (H_2L = *N*,*N*′-bis(5-bromo-3-methoxysalicylidene)phenylene-1,2-diamine). The X-ray structure of **1** (Figure 1) revealed a centrosymmetric core with two equivalent Eu_2L moieties linked by two μ-Cl^- ions and two μ_3-OH^- ions. For each Eu_2L moiety, the two Eu^{3+} ions are coordinated to the N_2O_2 and O_2O_2 binding sites, although they are located well outside of the overall plane of the ligand (Eu···N_2O_2 = 1.494 Å, Eu···O_2O_2 = 0.979 Å). Eu(1) is 8-coordinate, while Eu(2) is 9-coordinate. Eu(1) and Eu(2A) are linked by one Cl^- anion and one μ_3-OH^- ion with a separation of 4.087 Å.

Reaction of **1** with 1,4-H_2BDC in a 1:1 mole ratio in MeOH gave **2** in 60% yield. A view of the cationic complex is shown in Figure 2. The formation of **2** is accomplished by the insertion of 1,4-BDC units between two Eu_2L moieties of **1**. The overall structure of **2** comprises two crystallographically equivalent Eu_4L_2 units related by a center of symmetry and linked by two 1,4-BDC groups. Instead of a parallel configuration as in the $[Zn_4Nd_2L_4(1,4\text{-BDC})_2]^{2+}$ prism,[4] the 1,4-BDC units are virtually perpendicular to each other which results in the cagelike structure. The complex is of nanoscale proportions (17.5 × 17.3 × 10.8 Å). Each

Table 3. Selected Bond Lengths (Å) and Angles (deg) for **2**

Eu(1)−O(3)	2.357(8)	O(3)−Eu(1)−O(2)	66.0(2)
Eu(1)−O(2)	2.379(7)	O(3)−Eu(1)−O(1)	125.1(3)
Eu(1)−O(5)	2.478(8)	O(2)−Eu(1)−O(1)	61.0(3)
Eu(1)−O(6)	2.507(7)	O(3)−Eu(1)−O(4)	62.1(3)
Eu(1)−O(1)	2.586(10)	O(2)−Eu(1)−O(4)	125.2(3)
Eu(1)−O(4)	2.624(8)	O(1)−Eu(1)−O(4)	150.6(3)
Eu(2)−O(2)	2.310(7)	O(2)−Eu(2)−O(3)	67.4(3)
Eu(2)−O(3)	2.338(7)	O(2)−Eu(2)−N(2)	110.1(3)
Eu(2)−O(6)	2.369(7)	O(3)−Eu(2)−N(2)	73.0(3)
Eu(2)−N(2)	2.493(9)	O(2)−Eu(2)−N(1)	73.0(3)
Eu(2)−N(1)	2.498(9)	O(3)−Eu(2)−N(1)	103.8(3)
Eu(3)−O(2′)	2.382(7)	N(2)−Eu(2)−N(1)	63.8(3)
Eu(3)−O(3′)	2.401(7)	O(2′)−Eu(3)−O(3′)	65.0(2)
Eu(3)−O(7)	2.452(7)	O(2′)−Eu(3)−O(4′)	126.4(2)
Eu(3)−O(8)	2.503(7)	O(3′)−Eu(3)−O(4′)	63.7(3)
Eu(3)−O(4′)	2.537(8)	O(2′)−Eu(3)−O(1′)	61.8(2)
Eu(3)−O(1′)	2.580(8)	O(3′)−Eu(3)−O(1′)	124.1(2)
Eu(4)−O(3′)	2.265(7)	O(4′)−Eu(3)−O(1′)	148.3(2)
Eu(4)−O(2′)	2.365(7)	O(3′)−Eu(4)−O(2′)	67.4(2)
Eu(4)−O(8)	2.377(7)	O(3′)−Eu(4)−N(1′)	107.8(3)
Eu(4)−N(1′)	2.441(9)	O(2′)−Eu(4)−N(1′)	72.2(3)
Eu(4)−N(2′)	2.510(8)	O(3′)−Eu(4)−N(2′)	73.2(3)
		O(2′)−Eu(4)−N(2′)	104.4(2)
		N(1′)−Eu(4)−N(2′)	62.5(3)

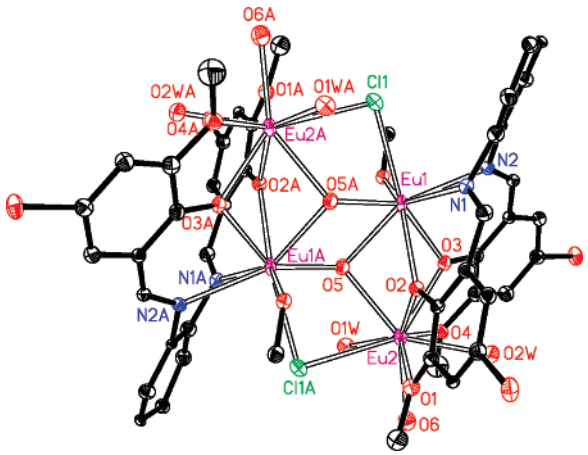

Figure 1. X-ray structure of the tetrameric unit of **1**. Thermal ellipsoids are drawn at the 25% probability level.

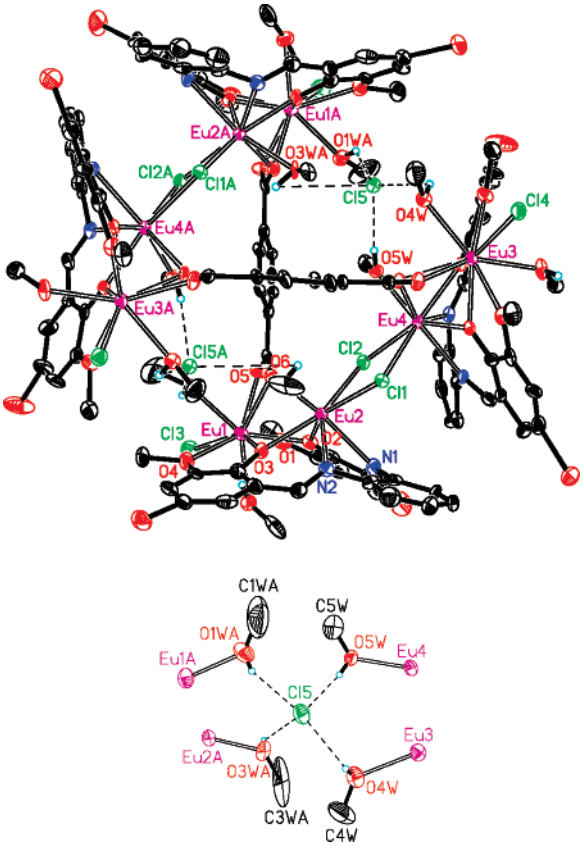

Figure 2. X-ray structure of **2** (above) and a detailed view of the unique encapsulated Cl^- anion (bottom). Thermal ellipsoids are drawn at the 25% probability level.

Eu_4L_2 unit consists of two similar Eu_2L moieties bridged by two μ-Cl groups. For each Eu_2L moiety, the two Eu^{3+} ions are coordinated to the N_2O_2 and O_2O_2 binding sites as those in **1**, and they are also located outside of the overall plane of the ligand (Eu···N_2O_2 = 1.440 Å, Eu···O_2O_2 = 0.973 Å (av)). In addition to the Schiff base and 1,4-BCD ligands, each of the O_2O_2-bound Eu(III) ions (Eu(1) and Eu(3)) bears two MeOH groups and a terminal chloride. The inner bound N_2O_2 Eu(III) ions (Eu(2) and Eu(4)) also bear a single MeOH.

The orientation of four Eu-bound MeOH groups within the cage permits an interesting mode of anion binding. Two chloride ions, equivalent by the center of symmetry, are encapsulated within the cage and each is bound via four Cl···H−OMe hydrogen bonds (Cl···O = 3.056−3.118 Å) (Figure 2). These interactions may play a role in a self-assembly process of cage formation during crystallization because, in solution (MeOH or MeCN), the molar conductivity studies are consistent with a 4:1 electrolyte indicating that the two encapsulated Cl^- anions separate from the cage structure. In the solid-state, two additional unbound, non-encapsulated Cl^- ions are located outside the cage structure and fulfill the remaining valence requirements of the Eu_8 cluster. The ^{1}H NMR spectra of **2** in CD_3CN at room temperature show 26 slightly broadened peaks ranging from −11 to +24 ppm which remain unchanged over several weeks (see Figure S1, Supporting Information).

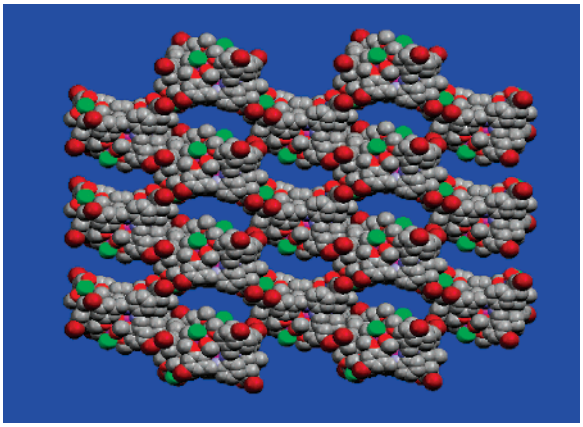

Figure 3. Space filling view of **2** along the *a*-axis showing the open mesoporous structure.

In the solid state, **2** has an open, porous 3D metal−organic framework architecture formed by supramolecular interactions between neighboring Eu_8L_4 moieties (Figure 3). Thus, along the *c*-axis, a one-dimensional zigzag configuration of Eu_8 clusters is generated by the presence of two Cl···H−OMe hydrogen-bonded interactions between terminal chloride and MeOH groups (Cl···O = 3.029 Å) (see Figure S3). Each of these strands is further connected to four neighbors via intermolecular $\pi-\pi$ stacking interactions (center-to-center distances of 3.595 Å av, see Figure S2). The resulting porous structure has extended channels running along both the *a*- and *c*- axes. These channels measure approximately 8 × 15 and 7 × 18 Å, respectively, and accommodate guest molecules of MeOH and H_2O (see Figure S4). Hydrogen-bonded interactions are present between the entrapped molecules and the surrounding supramolecular framework.

Quartz Crystal Microbalance (QCM) Studies of 2. We have studied the reversible host−guest binding of MeOH by **2** using the gas-phase quartz crystal microbalance (QCM) technique, a proven nanogravimetric method for the detection of the gas phase insertion and removal of VOCs from a host material.[9] Figure 4 is a plot of the apparent partition coefficient versus normalized partial pressure and shows binding site saturation, qualitatively consistent with the Langmuir isotherm model. Nonselective binding would have resulted in a more-linear response characteristic of weak physical interactions (van der Waals forces).[10] Interestingly, the partition coefficient of **2** at saturation is approximately 13.7, which is significantly lower than the K_{app} values of many other host materials. Although the calculated channel sizes are large enough to accommodate the physical insertion of MeOH into the pores of **2**, we hypothesize that partitioning is hindered because of the hydrogen-bonding interactions that cause MeOH to preferentially interact at (or just inside) channel entrances, creating a transport bottleneck for the additional uptake of MeOH.

Spectroscopic Studies. The photophysical properties of **1** and **2** were studied in CH_3CN, CH_3OH, and CD_3OD. The

(9) Yang, X.-P.; Hahn, B. P.; Jones, R. A.; Stevenson, K. J.; Swinnea, J. S.; Wu, Q. *Chem. Commun.* **2006**, 3827−3829 and references therein.
(10) Pinalli, R.; Suman, M.; Dalcanale, E. *Eur. J. Org. Chem.* **2004**, 451.

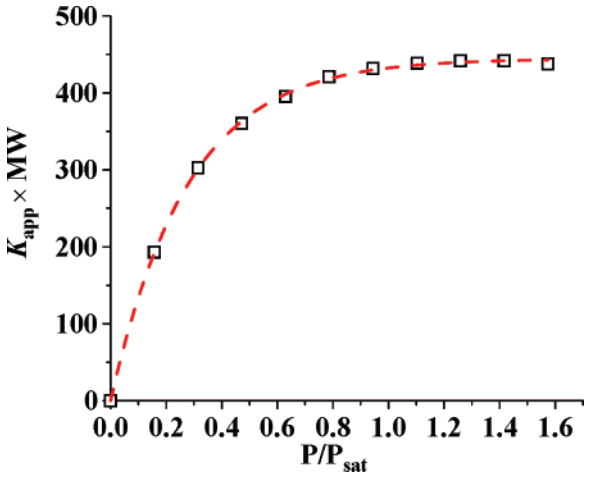

Figure 4. Apparent partition coefficient vs normalized partial pressure of MeOH for **2**.

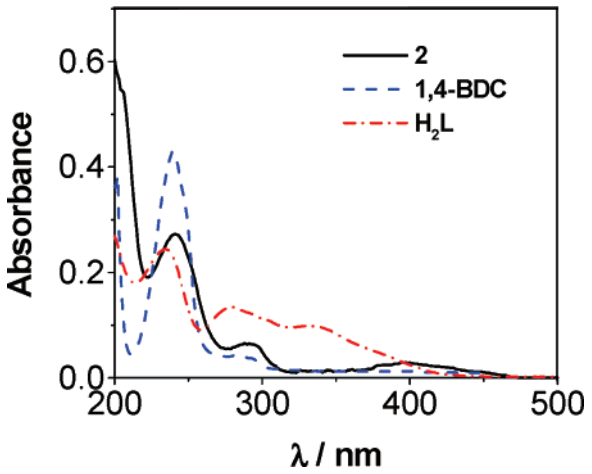

Figure 5. Absorption spectra of the free ligand H_2L, 1,4-BDC, and **2**.

free ligand H_2L exhibit absorption bands at 228, 260, and 336 nm, and 1,4-BDC exhibits a band at 240 nm; all of these bands are red shifted upon coordination to the metal ion in both **1** and **2** (Figure 5). The emission spectrum of the free ligand H_2L and the excitation and emission spectra of **2** are shown in Figure 6. Excitation of the absorption band at 279 nm of the free H_2L produces a broad emission band at λ_{max} = 468 nm. Upon excitation of the ligand-centered absorption bands, both **1** and **2** show typical visible emission bands of the Eu^{3+} ion ($^5D_0 \rightarrow {}^7F_j$ transitions, j = 0, 1, 2, 3 and 4), while the ligand centered (L or 1,4-BDC) $^1\pi-\pi^*$ emissions were not detected. The fluorescence quantum yields (Φ_{em}) in CH_3CN, CH_3OH, and CD_3OD are 0.093, 0.040, and 0.065 for **1** and 0.126, 0.071, and 0.135 for **2**, respectively.[11] For either **1** or **2**, the quantum yields in CH_3CN and CD_3OD are higher than that in CH_3OH. This is probably because of an exchange between coordinated MeOH with these solvents.[12] It is noteworthy that, in the same solvent, the fluorescence quantum yield of **2** is higher than that of **1**. This difference in luminescence may be caused by the different Eu^{3+} environments in **1** and **2**. In **2**, the Eu^{3+} ions are enclosed by two kinds of chromophoric ligands (L and 1,4-BDC) and are fairly well protected in the cage. In **1**, the Eu^{3+} ions are considerably more exposed to potential interactions with solvent molecules.

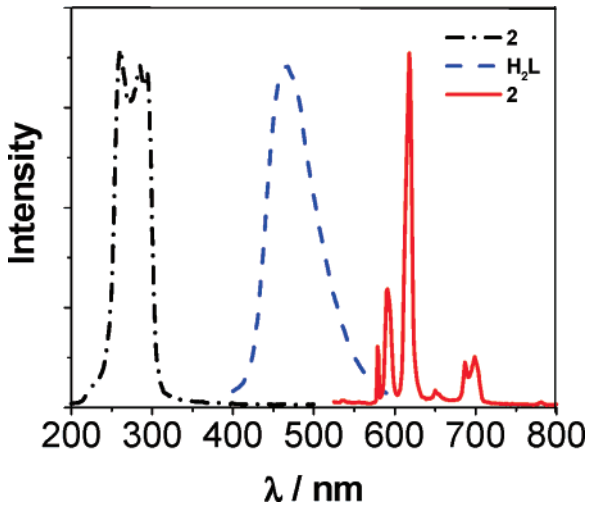

Figure 6. Excitation spectrum of **2** and emission spectra of the free ligand H_2L and **2** in CH_3OH.

Conclusions

In conclusion, we have successfully demonstrated the application of a "two-ligand" approach to the construction of functional polynuclear lanthanide complexes and discovered a very unusual mode of anion binding within a Eu_8 cage structure. To the best of our knowledge, the octanuclear Eu(III) complex **2** is the highest nuclearity lanthanide salen complex reported until now. It exhibits an open porous three-dimensional metal−organic framework structure and shows better luminescence properties than its precursor **1**. Further studies focused on this synthetic methodology and the improvement in luminescence properties by the construction of novel high-nuclearity lanthanide clusters are in progress.

Acknowledgment. We thank the Robert A. Welch Foundation (Grants F-816 and F-1529), the Hong Kong Baptist University (FRG/03-04/II-52), and the Hong Kong Research Grants Council (HKBU 2038/02P) for support.

Supporting Information Available: ^1H NMR spectrum of **2** in CD_3CN, figures of **2** in the solid state, and X-ray crystallographic data for **1** and **2** (CIF). This material is available free of charge via the Internet at http://pubs.acs.org. Crystallographic information is available upon request from the Cambridge Crystallographic Data Centre under numbers CCDC-644264 (**1**) and 644265 (**2**) (www.ccdc.cam.ac.uk).

IC7008682

(11) Fluorescence quantum yields were determined relative to $[Ru(bipy)_3]Cl_2$ in water (bipy = 2,2′-bipyridine, Φ_{em} = 0.028): Nakamaru, K. *Bull. Soc. Chem. Jpn.* **1982**, *5*, 2697.
(12) Sabbatini, N.; Guardigli, M.; Lehn, J. M. *Coord. Chem. Rev.* **1993**, *123*, 201.